

Arbitrary Order Aberrations for Elements Characterized by Measured Fields

Kyoko Makino and Martin Berz

Department of Physics and Astronomy and National Superconducting Cyclotron Laboratory,
Michigan State University, East Lansing, Michigan 48824 USA

ABSTRACT

The precise understanding of the properties of large acceptance devices like modern nuclear spectrographs often requires the calculation of high-order aberrations. In many practical cases, it is necessary to treat all details of the fields of the elements, and instead of utilizing more or less simple field models, one has to rely on measured data. It is shown how aberrations of in principle unlimited orders can be obtained from measured field data; moreover, for the remaining aberrations of yet higher order, rigorous upper bounds of their influence on the motion can be found. The methods are used for the analysis and correction of the high-resolution S800 spectrograph at MSU.

Keywords: Transfer map, High order aberrations, Differential Algebras, Remainder-enhanced Differential Algebras, Taylor model, COSY INFINITY, Fringe field, Measured field, Wavelet representation, Spectrograph

1. INTRODUCTION

The approach of transfer maps has been widespread in the design and study particle optical systems such as accelerators, spectrometers, beamlines, electron microscopes as well as glass optical system. Combined with the differential algebraic (DA) techniques,¹⁻⁴ computation of Taylor maps to high order have been performed extensively. The higher-order aberrations obtained in this approach offer a more efficient analysis of the particle optical systems, and hence often simplify the design of a system.

One of the crucial particle optical systems which require the knowledge of high order aberrations are modern high resolution spectrographs for nuclear physics. Their large phase space acceptance sometimes turns out to demand a careful study of higher order aberrations up to seventh order.⁵ To this end, the most critical question is that the simulation treats the field as precisely as possible. Since such spectrographs use large aperture magnets, a careful consideration of the fringe fields is indispensable. Some efficient methods to take account of the fringe field were discussed in Refs. 6,7 in detail. In this paper, we will discuss the technique to compute transfer maps for measured fields in the framework of DA methods. The technique supplies more precise information of the system, which cannot be obtained otherwise. The method has been implemented in the DA-based code COSY INFINITY,^{8,9} and has been used for the simulations of various spectrographs, including the S800 Spectrograph¹⁰ at the National Superconducting Cyclotron Laboratory at Michigan State University and the spectrographs at Jefferson Laboratory. Figure 1 shows the measured field data of a bending magnet of the S800 Spectrograph,¹¹ and these field data are used for the computation of the transfer map of the system.

Another important question is how to treat errors unavoidably associated to measurement and computation. A new technique, the method of Remainder-enhanced Differential Algebras (RDA), enables to express a function by a Taylor polynomial and an interval error bound of the Taylor remainder. The error bounds are usually rather sharp especially at higher orders.¹²⁻¹⁶ A verified integration scheme^{17,16} in the framework of RDA makes it possible to obtain Taylor transfer maps with rigorous remainder error bound for any arbitrary element including a measured field element. The RDA method also has been implemented in COSY INFINITY.

Other author information:

K. M.: Email: makino@nscl.msu.edu; WWW: <http://www.beamtheory.nscl.msu.edu/>; Telephone: 517-333-6441; Fax: 517-353-5967.
M. B.: Email: berz@pa.msu.edu; WWW: <http://www.beamtheory.nscl.msu.edu/>; Telephone: 517-333-6313; Fax: 517-353-5967.

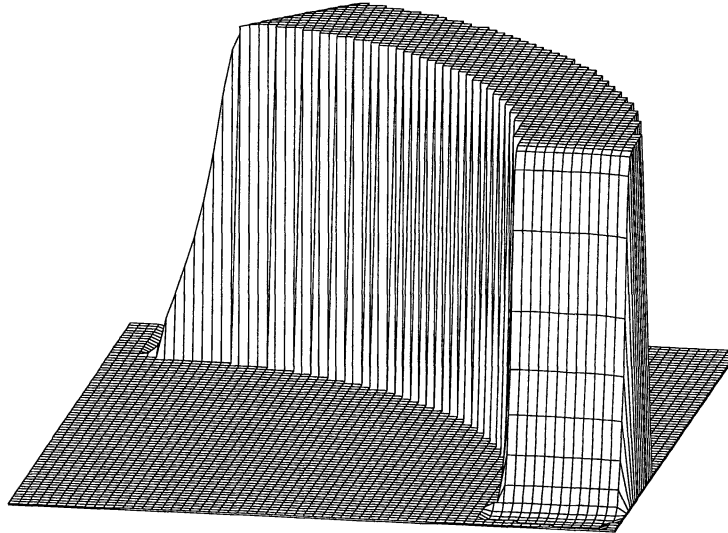


Figure 1. The measured field of a bending magnet of the S800 Spectrograph. The measured data is supplied at 328×370 points. The above picture shows the field at 65×74 points.

2. WAVELET REPRESENTATION

For the purpose of including measured field data as a part of a particle optical system, a good interpolation method is required to obtain a field value from the limited information contained in the measured field data. The interpolation method has to fit to the DA technique, and in particular the result of the interpolation has to be differentiable as often as needed. Also the capability of localization by the approach of wavelets¹⁸ is very useful for our purpose. Since our target data is more or less smooth as shown in Figure 1, we chose the method of Gaussian wavelets, which assures the required differentiability.

Assume a set of data Y_i is given at N equi-distant points x_i for $i = 1, \dots, N$. Then, the interpolated value at a point x is expressed as

$$V(x) = \sum_{i=1}^N Y_i \frac{1}{\sqrt{\pi}S} \exp \left[-\frac{(x - x_i)^2}{\Delta x^2 S^2} \right],$$

where Δx is the distance of two neighbouring points x_i and x_{i+1} , and S is the factor to control the width of Gaussian wavelets.

Table 1. Accuracy of the Gaussian wavelets representation for one dimensional functions.

Test Function	Number of Gaussian Wavelets N	Average Error	Maximum Error
1	10	2.6×10^{-14}	2.6×10^{-14}
$x + 1$	10	1.5×10^{-14}	2.6×10^{-14}
$\cos(x) + 1$	400	6.3×10^{-5}	1.0×10^{-4}
$\exp(-x^2)$	600	4.6×10^{-5}	1.6×10^{-4}

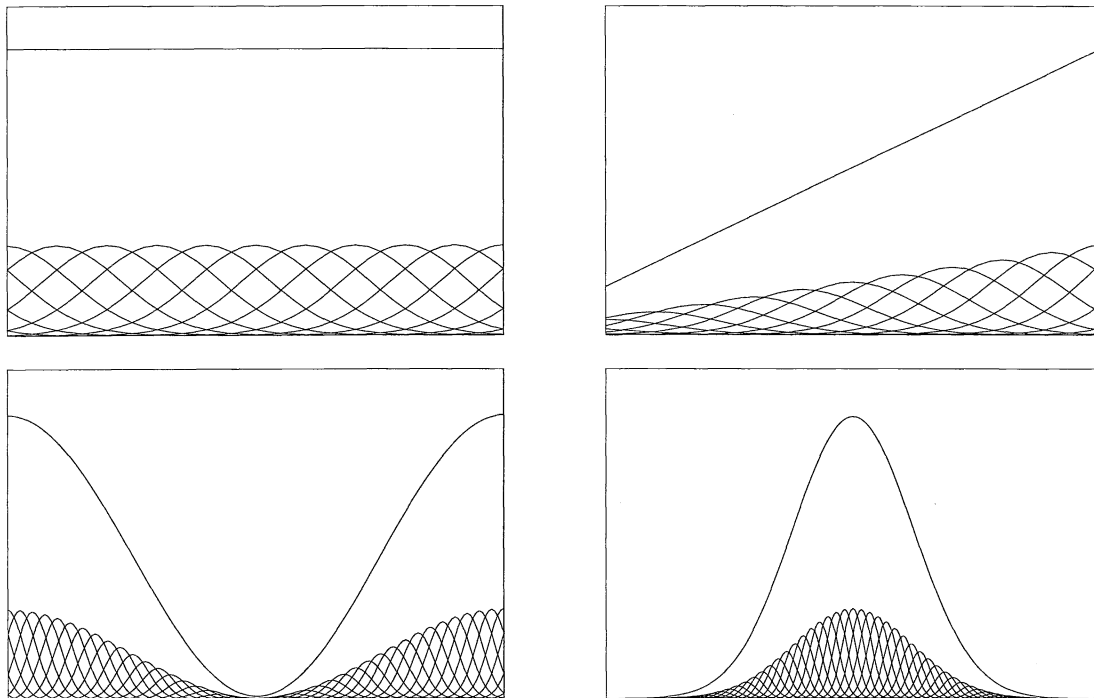


Figure 2. The Gaussian wavelets representation for $f(x) = 1$ (top left), $f(x) = x + 1$ (top right), $f(x) = \cos x + 1$ (bottom left) and $f(x) = \exp(-x^2)$ (bottom right).

Figure 2 shows how the Gaussian interpolation as a sum of Gaussian wavelets works for several one dimensional functions, including linear functions, a trigonometric function and a Gaussian function. The data values Y_i are supplied by taking their function values at each point x_i to simulate the function. Proportional to each height of the data Y_i , a Gaussian wavelet $\exp[-(x - x_i)^2 / \Delta x^2 S^2]$ is placed at x_i . The resulting interpolated function is shown in each picture, which represents the original function very well. S is chosen to be 1.8 for all the cases. Table 1 summarizes the accuracy of the method for those functions. Note that in this approach, the main emphasis is not necessarily to model the function as accurately as possible, but the scaling of the height with function values provides a method that also allows smoothing of potentially noisy data for larger values of S . Figure 3 shows the behavior of derivatives of interpolated functions up to third order. As an example, the Gaussian function $f(x) = \exp(-x^2)$ is chosen to be the original function shape.

The advantage of the Gaussian function and many other wavelets is that it falls off quickly. Thus the potentially time consuming summation over all wavelets can be replaced by the summation of only the neighboring Gaussian wavelets in the range of $\pm 5S$, which is in the vein of other wavelet transforms and greatly improves efficiency.

3. ELEMENTS CHARACTERIZED BY MEASURED FIELDS

The Gaussian wavelets representation discussed above is utilized to represent fields which are specified by measured data. Because of the favorable features of the Gaussian function, the method allows the computation of the transfer map of such a magnetic field element. In fact, because it is possible to determine the field everywhere from just the knowledge of the field in the midplane,¹⁹ it is sufficient to supply only two dimensional midplane measured data.

Similar to the procedure discussed in the previous section, the measured field data is given at equi-distant grid points in two dimensional cartesian coordinates. Figure 4 shows how the data grid is specified and the cartesian coordinate corresponding to the data grid. Assume a set of data $BY(i_x, i_z)$ is given at equi-distant $N_x \times N_z$ points

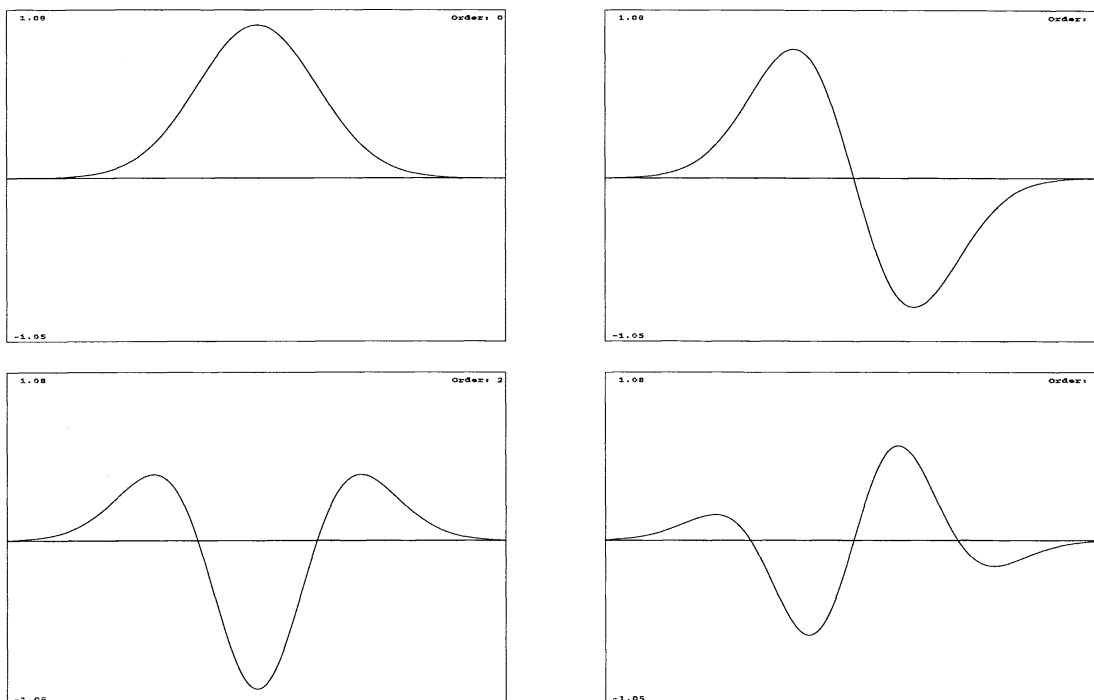


Figure 3. The derivatives of the function $f(x) = \exp(-x^2)$ when represented by an ensemble of Gaussian wavelets. The top left shows the interpolated function, the top right shows the first order derivative of the interpolated function, the bottom left is the second order derivative and the bottom right is the third order derivative.

(x_{i_x}, z_{i_z}) for $i_x = 1, \dots, N_x, i_z = 1, \dots, N_z$. Then, the interpolated value at a point (x, z) is expressed as

$$B_y(x, z) = \sum_{i_x=1}^{N_x} \sum_{i_z=1}^{N_z} BY(i_x, i_z) \frac{1}{\pi S^2} \exp \left[-\frac{(x - x_{i_x})^2}{\Delta x^2 S^2} - \frac{(z - z_{i_z})^2}{\Delta z^2 S^2} \right],$$

where Δx and Δz are the grid spacing in x and z directions, respectively, and S is the control factor of the width of Gaussian wavelets.

A suitable choice of the control factor S depends on the behaviour of the original supplied data. If S is too small, the mountain structure of individual Gaussian wavelets is observed. On the other hand, if S is too large, the original value supplied by the data is washed out, which can also be used effectively for purposes of smoothing. For constant fields, the suitable S is about 1.8. For quickly varying fields, it should be about 1.0. Larger values of S usually provide more accurate evaluation of the derivatives.

The code COSY INFINITY⁸ contains a particle optical element to compute the transfer map from measured field data. For the purpose to specify the position of the particle in the element, the starting point (S_x, S_z) and the direction S_ϕ of the trajectory of reference particle have to be given as shown in Figure 4.

4. EXAMPLE - THE S800 SPECTROGRAPH

The element discussed above is used especially often to study and design spectrographs. In this section, we will use the S800 Spectrograph¹⁰ at the National Superconducting Cyclotron Laboratory at Michigan State University as an example. The system parameters of the S800 Spectrograph are listed in Table 2.

For the purpose of comparison, we made several computations using the code COSY INFINITY. They are based on

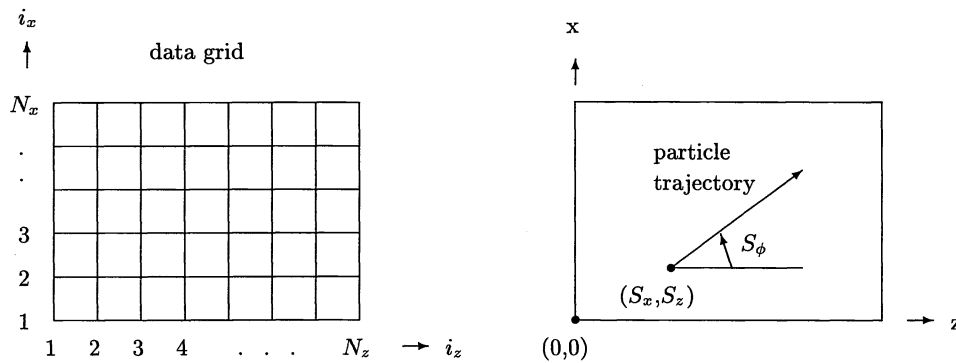


Figure 4. The specification of measured field data for a particle optical element.

Table 2. The layout of the S800 Spectrograph.

Drift	$l = 60$ cm				
Quad	$l = 40$ cm	$G_{max} = 21$ T/m	$r = 0.1$ m		
Drift	$l = 20$ cm				
Quad	$l = 40$ cm	$G_{max} = 6.8$ T/m	$r = 0.2$ m		
Drift	$l = 50$ cm				
Dipole	$\rho = 2.675$ m	$B_{max} = 1.5$ T	$\phi = 75^\circ$	$\epsilon_1 = 0^\circ$	$\epsilon_2 = 30^\circ$
Drift	$l = 140$ cm				
Dipole	$\rho = 2.675$ m	$B_{max} = 1.5$ T	$\phi = 75^\circ$	$\epsilon_1 = 30^\circ$	$\epsilon_2 = 0^\circ$
Drift	$l = 257.5$ cm				

- Homogeneous dipoles without fringe field consideration.
- Inhomogeneous dipoles that take into account the slight inhomogeneities extracted from measurements, but have no fringe field consideration.
- Inhomogeneous dipoles with fringe field consideration using a model based on Enge functions.^{6,7}
- Utilizing actual measured field data for the first of the dipoles.

The initial design of the system listed in Table 2 was made without using the measured field data element. The computation of the transfer maps show differences between the model with the measured field data element and the others. As shown in Figure 5, the off-energy rays in the idealized S800 system focus on the final plane, while the S800 system in which one dipole magnet was replaced by the measured field data element does not quite produce a focus at the end any more. Table 3 shows several characteristic aberrations computed in the various ways as mentioned above.

In order to obtain a fully accurate model of the S800 spectrograph, also measurements of the second dipole will be utilized once they will be available. Furthermore, it is expected that subsequent measurements will have less noise than the currently available data, which should be able to improve the overall field representation, require less smoothing, and allows to utilize narrower Gaussian wavelets. For the process of obtaining bounds for the Taylor remainders, the verified integrators discussed in^{17,16} as well as overall field error estimates will be utilized.

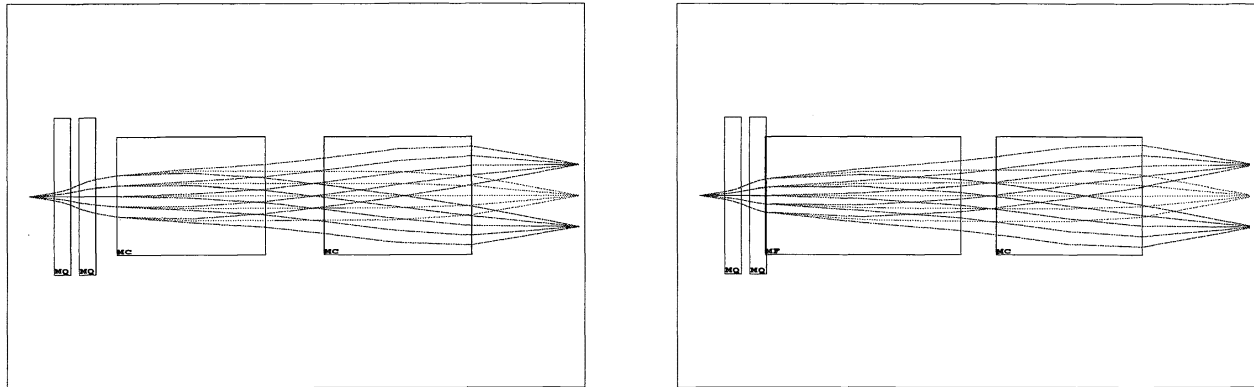


Figure 5. The off-energy rays of the S800 system without (left) and with (right) the measured field data element.

Table 3. Some characteristic aberrations of the S800 Spectrograph.

Aberrations	Homogeneous Dipoles without fringe field	Inhomogeneous Dipoles without fringe field	Inhomogeneous Dipoles with fringe field	Measured Field Dipole and Inhomogeneous dipole with fringe field
(x, x)	0.8322	0.8322	0.8322	0.7103
(x, a)	-0.0213	-0.0213	-0.0207	-0.1616
(x, δ)	4.9266	4.9266	4.9222	4.9252
(x, aa)	-3.7328	-4.9459	-4.9316	-3.3508
$(x, a\delta)$	-4.7288	-3.5688	-3.5818	-3.9811

ACKNOWLEDGEMENTS

We are grateful for the financial support of this research to the Department of Energy, Grant No. DE-FG02-95ER40931, and the Alfred P. Sloan Foundation.

REFERENCES

1. M. Berz, "Differential algebraic description of beam dynamics to very high orders," *Particle Accelerators* **24**, p. 109, 1989.
2. M. Berz, "Arbitrary order description of arbitrary particle optical systems," *Nuclear Instruments and Methods* **A298**, p. 426, 1990.
3. M. Berz, *High-Order Computation and Normal Form Analysis of Repetitive Systems*, in: M. Month (Ed), *Physics of Particle Accelerators*, vol. AIP 249, p. 456. American Institute of Physics, 1991.
4. M. Berz, "Modern map methods for charged particle optics," *Nuclear Instruments and Methods* **363**, p. 100, 1995.
5. M. Berz, K. Joh, J. A. Nolen, B. M. Sherrill, and A. F. Zeller, "Reconstructive correction of aberrations in nuclear particle spectrographs," *Physical Review C* **47,2**, p. 537, 1993.
6. G. H. Hoffstätter, *Rigorous bounds on survival times in circular accelerators and efficient computation of fringe-field transfer maps*. PhD thesis, Michigan State University, East Lansing, Michigan, USA, 1994. also DESY 94-242.
7. G. Hoffstätter and M. Berz, "Symplectic scaling of transfer maps including fringe fields," *Physical Review E* **54,4**, 1996.

8. M. Berz, "COSY INFINITY Version 7 reference manual," Tech. Rep. MSUCL-977revised, National Superconducting Cyclotron Laboratory, Michigan State University, East Lansing, MI 48824, 1996. see also <http://www.beamtheory.nsl.msu.edu/cosy/>.
9. K. Makino and M. Berz, "COSY INFINITY version 7," in *Fourth Computational Accelerator Physics Conference*, AIP Conference Proceedings, 1996.
10. J. Nolen, A. Zeller, B. Sherrill, J. C. DeKamp, and J. Yurkon, "A proposal for construction of the S800 spectrograph," Tech. Rep. MSUCL-694, National Superconducting Cyclotron Laboratory, 1989.
11. J. A. Caggiano and B. Sherrill, "Data analysis techniques for S800 dipole magnetic field maps." Annual Report of the Michigan State University National Superconducting Cyclotron Laboratory, 1995.
12. K. Makino and M. Berz, "Remainder differential algebras and their applications," in: *Computational Differentiation: Techniques, Applications, and Tools SIAM*, 1996.
13. M. Berz, "From Taylor series to Taylor models," in *Proceedings, First Accelerator Theory Institute*, AIP, 1997.
14. K. Makino and M. Berz, "Implementation and applications of Taylor model methods," *Reliable Computing submitted*, 1997.
15. K. Makino, "Rigorous integration of maps and long-term stability," in *Proceedings, 1997 Particle Accelerator Conference*, vol. in print, APS, 1997.
16. M. Berz and K. Makino, "Arbitrary order maps, remainder terms, and long term stability in particle accelerators," in *these proceedings, Optical Science, Engineering and Instrumentation '97*, SPIE, 1997.
17. M. Berz and K. Makino, "Integration of ODEs and flows with differential algebraic methods on Taylor models," *Reliable Computing submitted*, 1997.
18. I. Daubechies, *Ten Lectures on Wavelets*, SIAM, Philadelphia, 1992.
19. M. Berz, "Computational aspects of design and simulation: COSY INFINITY," *Nuclear Instruments and Methods A298*, p. 473, 1990.